



NRC Publications Archive Archives des publications du CNRC

Frequency analysis of temperature-dependent interferometric signal for the measurement of the temperature coefficient of refractive index

Zhou, Jianqin; Shen, Jun; Neill, W. Stuart

This publication could be one of several versions: author's original, accepted manuscript or the publisher's version. / La version de cette publication peut être l'une des suivantes : la version prépublication de l'auteur, la version acceptée du manuscrit ou la version de l'éditeur.

For the publisher's version, please access the DOI link below. / Pour consulter la version de l'éditeur, utilisez le lien DOI ci-dessous.

Publisher's version / Version de l'éditeur:

<https://doi.org/10.1063/1.4958820>

Review of Scientific Instruments, 87, 7, 2016-07-19

NRC Publications Record / Notice d'Archives des publications de CNRC:

<https://nrc-publications.canada.ca/eng/view/object/?id=c0eb6f16-89d8-4e81-b014-0c8387a943e1>

<https://publications-cnrc.canada.ca/fra/voir/objet/?id=c0eb6f16-89d8-4e81-b014-0c8387a943e1>

Access and use of this website and the material on it are subject to the Terms and Conditions set forth at

<https://nrc-publications.canada.ca/eng/copyright>

READ THESE TERMS AND CONDITIONS CAREFULLY BEFORE USING THIS WEBSITE.

L'accès à ce site Web et l'utilisation de son contenu sont assujettis aux conditions présentées dans le site

<https://publications-cnrc.canada.ca/fra/droits>

LISEZ CES CONDITIONS ATTENTIVEMENT AVANT D'UTILISER CE SITE WEB.

Questions? Contact the NRC Publications Archive team at

PublicationsArchive-ArchivesPublications@nrc-cnrc.gc.ca. If you wish to email the authors directly, please see the first page of the publication for their contact information.

Vous avez des questions? Nous pouvons vous aider. Pour communiquer directement avec un auteur, consultez la première page de la revue dans laquelle son article a été publié afin de trouver ses coordonnées. Si vous n'arrivez pas à les repérer, communiquez avec nous à PublicationsArchive-ArchivesPublications@nrc-cnrc.gc.ca.



Frequency Analysis of Temperature-dependent Interferometric Signal for the Measurement of the Temperature Coefficient of Refractive Index

Jianqin Zhou ^{a,*}, Jun Shen ^a, W. Stuart Neill ^b,

^a National Research Council of Canada, Energy, Mining and Environment Portfolio, 4250 Wesbrook Mall, Vancouver, British Columbia, Canada V6T 1W5

^b National Research Council of Canada, Energy, Mining and Environment Portfolio, 1200 Montreal Rd, Ottawa, Ontario, Canada K1A 0R6

Abstract

A method of frequency analysis for the measurement of the temperature coefficient of refractive index (dn/dT) using a Fabry–Perot interferometer was developed and tested against ethanol and water. The temperature-dependent interferometric signal described by Airy's formula was analyzed in both the temperature and frequency domains. By fast Fourier transform (FFT), a low-pass filter was designed and employed to eliminate the noise superimposed on the signal. dn/dT was determined accurately from the noise-removed signal by peak analysis. Furthermore, the signal frequency parameters may be utilized for material thermophysical property characterization. This method lays the foundation for an on-line dn/dT instrument for monitoring chemical processes.

Keywords: Temperature coefficient of refractive index; Peak analysis; Frequency analysis; Noise reduction

* Corresponding author. Fax: +1 604 221 3001.
E-mail address: jianqin.zhou@nrc-cnrc.gc.ca (J. Zhou).

1. Introduction

The temperature coefficient of refractive index (dn/dT) is an important parameter for material thermophysical property characterization. For example, dn/dT may be used to evaluate hydrocarbon fuel quality. It was reported that dn/dT can be utilized to discriminate biodiesels produced by transesterification using ethanol and methanol [1]. A recent study [2] on refinery streams revealed that dn/dT is clearly correlated to several important fuel properties. The refinery streams with a lower cetane number, lower distillation temperatures (T50, T90) and lower viscosity had a higher $-dn/dT$ value. Correlations of $-dn/dT$ with distillation temperatures and viscosity can be attributed to the dependence of this property on molecular size (or weight) [2, 3].

Several methods, such as optical interferometer technique [4, 5], thermal lens spectrometry [6, 7], and minimum deviation method [8], can be used for dn/dT measurement. Optical interferometer is a low-cost and easy-to-perform technique and has been widely applied [2-5]. It includes a heating device that induces a slow and uniform temperature variation in a sample, causing the intensity of interference fringe to change. The intensity is recorded against temperature as a temperature-dependent interferometric signal. In peak analysis, each temperature T corresponding to a signal peak is extracted and assigned with an interference order m to attain an m - T curve and its derivative dm/dT , from which, dn/dT can be deduced. In practice, the recorded interferometric signal is affected by noise, such as air turbulence, environmental vibration, or instrument noise. This leads to false peaks in the signal and thus error data in the m - T curve and dm/dT . Decreasing signal sampling rate may reduce signal false peaks [3, 5]. However, because

the noise was randomly distributed, a manual false peak removal was often required even at lower sampling rate.

To remove the noise from the signal, in this work, a method of frequency analysis was developed and tested against ethanol and water. By fast Fourier transform (FFT), a low-pass filter could be designed and employed to eliminate the noise superimposed on the signal. From the noise-removed signal, dn/dT values could be acquired accurately by peak analysis. Furthermore, the frequency parameters derived from the frequency analysis could be used for material thermophysical property characterization.

2. Optical Interferometer Technique

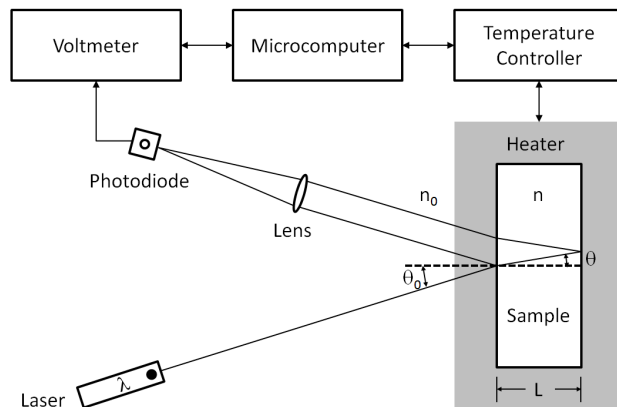


Figure 1 The principle of a Fabry-Perot interferometer and a schematic diagram of the experimental setup for dn/dT measurement

Fig. 1 shows the principle of a Fabry-Perot interferometer and a schematic diagram of the experimental setup for dn/dT measurement. The sample to be measured can be gas, liquid, or transparent solid material. The solid material can be made as a plate

with two parallel surfaces, while gas or liquid material can be enclosed in a transparent quartz cuvette with two parallel inner faces to form a plate. When a laser light is incident on the transparent plate, multiple reflections from the plate surfaces can create a multiple-beam interference fringe pattern described by Airy's formula [9]:

$$I_r = \frac{4R \sin^2(\delta/2)}{(1-R)^2 + 4R \sin^2(\delta/2)} I_i, \quad (1)$$

$$\delta = \frac{2\pi}{\lambda} \Delta s, \quad (2)$$

where λ is the wavelength of the laser light. I_i and I_r are the intensity of incident and reflected laser beams, respectively. R is the average reflectivity of the two parallel surfaces. δ is the phase difference induced by the difference of optical path length,

$$\Delta s = 2n(\lambda, T)L \cos \theta \cong 2n(\lambda, T)L \quad (\theta < 1^\circ). \quad (3)$$

Here L is the thickness of the plate, θ is the angle of refraction, and n is the refractive index of the material. For the convenience of discussion, the thermal expansion of solid material and the temperature effect of quartz cuvette containing gas or liquid material are not taken into consideration in Eq. (3) and will be discussed in detail in Section 4. For a given wavelength λ of the laser light, the refractive index of the material is a function of temperature T

$$n(\lambda, T) = n(T). \quad (4)$$

Defining the order of interference

$$m(T) = \frac{\delta}{2\pi} = \frac{\Delta s}{\lambda} = \frac{2L}{\lambda} n(T), \quad (5)$$

Eq. (1) can be expressed as

$$I_r(T) = \frac{F \sin^2[m(T)\pi]}{1 + F \sin^2[m(T)\pi]} I_i, \quad (6)$$

where

$$F = \frac{4R}{(1-R)^2}. \quad (7)$$

In this work, to measure the fringe intensity $I_r(T)$ with a liquid material, the liquid sample was contained in a transparent quartz cuvette ($L = 10 \text{ mm}$) with two parallel inner faces and irradiated by a weak He-Ne laser beam ($\lambda = 632.8 \text{ nm}$). Multiple reflections at both inner surfaces of the cuvette created an interference fringe pattern. A slow and uniform temperature variation was induced in the sample by an in-house made resistive heater controlled by a LakeShore 340 temperature controller. The heating of the sample caused a change of interference fringe intensity, which was detected by a photodiode and measured by a voltmeter (Agilent 34401A 6½ Digit Multimeter) as a temperature-dependent interferometric signal $I_r(T)$. Generally speaking, samples with positive or negative dn/dT will cause the interference fringe to move in opposite directions, which can be utilized to determine the sign of dn/dT . In the experiment, a known sample (e.g., ethanol) was measured first to determine the moving direction of a sample with negative dn/dT . Liquid hydrocarbons usually possess negative dn/dT [3].

3. Interferometric Signal Analysis

To explore the methodology for accurate dn/dT measurement, a finite discrete-temperature digital signal is generated to simulate the interferometric signal $I_r(T)$. The parameters of an N point temperature sequence are summarized in Table 1:

Table 1 The parameters of an N point temperature sequence

Temperature Range			Sample Number	Sample Interval	Signal Resolution	Highest Frequency	Frequency Resolution
T_0	T_N	$\Delta T = T_N - T_0$					

			N	$\delta_T = \Delta T/N$	$2\delta_T$	$1/2\delta_T$	$1/\Delta T$
25°C	35°C	10°C	5000	0.002 °C	0.004 °C	250 K ⁻¹	0.1 K ⁻¹

$$T = T_0 + j\delta_T = T_0 + j\frac{T_N - T_0}{N} \quad (j = 0, 1, \dots, N - 1), \quad (8)$$

A typical interference order, to a first approximation, is a single-variable quadratic function of temperature:

$$m(T) = c + bT + \frac{1}{2}aT^2 \quad (T_0 \leq T < T_N). \quad (9)$$

For a normalized simulation signal generated by Eq. (6):

$$I(T) = \frac{I_r(T)}{I_i} = \frac{F \sin^2[m(T)\pi]}{1 + F \sin^2[m(T)\pi]} \quad (T_0 \leq T < T_N), \quad (10)$$

the equation coefficients in Eq. (9) are chosen as $a = 0.1 \text{ K}^{-2}$, $b = 1.0 \text{ K}^{-1}$ and $c = -56.25$ to set $m(25^\circ\text{C}) = 0$. The average reflectivity R is chosen as 0.1 and F is about 0.5 [Eq. (7)]. The generated simulation signal is shown in Fig. 2.

(1) Signal Analysis

The fringe intensity $I(T)$ described by Airy's formula can be transformed to its interference order $m(T)$ by peak analysis. Referring to Eq. (10) and Fig. 2, when $m(T)$ varies with temperature, the maxima of $I(T)$ will appear at half-integral values ($m = \frac{1}{2}, 1\frac{1}{2}, 2\frac{1}{2}, \dots$) and minima at integral values ($m = 1, 2, 3, \dots$). Therefore, by extracting the temperature values at the maxima and minima of $I(T)$ and assigning $m(T)$ to each temperature value, $I(T)$ can be transformed to $m(T)$.

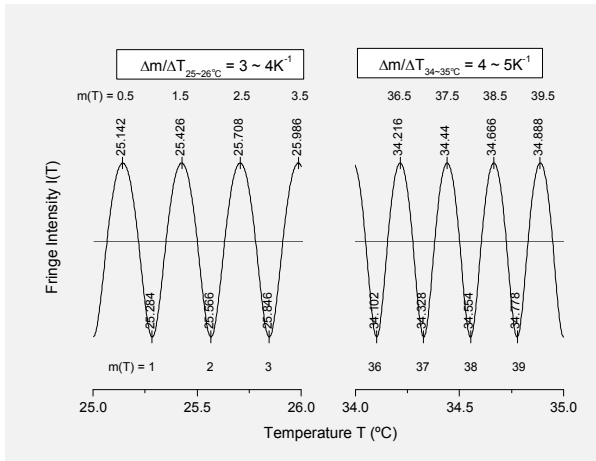


Figure 2 The generated simulation signal $I(T)$. The interference order $m(T)$ is assigned to the temperature values at the maxima and minima of $I(T)$

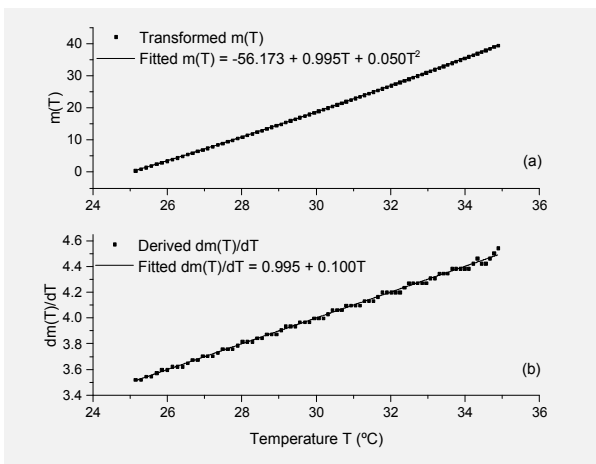


Figure 3 The transformed $m(T)$ and its first derivative $dm(T)/dT$

Fig. 3a presents the transformed interference order $m(T)$, which can be fitted to Eq. (9) by least-squares curve fitting to obtain equation coefficients. Fig. 3b shows the first derivative of the interference order $m' = dm/dT$, which is very important in the following aspects:

1. dm/dT is equal to signal frequency f — the number of peaks or valleys per unit temperature (Fig. 2)

$$f = m'. \quad (11)$$

For the simulation signal [Eq. (9)], we have the signal frequency

$$f = m' = b + aT = 1 + 0.1T \quad (T_0 \leq T < T_N), \quad (12)$$

the average frequency across the observation temperature range ($T_0 \leq T < T_N$)

$$\bar{f} = \bar{m}' = b + a\bar{T} = b + a\frac{T_0+T_N}{2} = 4K^{-1}, \quad (13)$$

and the frequency change across the observation temperature range ($T_0 \leq T < T_N$)

$$\Delta f = \Delta m' = a\Delta T = a(T_N - T_0) = 1K^{-1}. \quad (14)$$

2. dm/dT is proportional to the temperature coefficient of refractive index dn/dT [Eq.

(5)]

$$\frac{dn}{dT} = \frac{\lambda}{2L} m'. \quad (15)$$

Thus dn/dT can be calculated. For the experimental setup: $\lambda = 632.8 \text{ nm}$, $L = 10 \text{ mm}$

$$\frac{dn}{dT} = (0.3164 \times 10^{-4})m' \quad (16)$$

3. dm/dT is affected by limited sampling number of discrete signal and the noise in a practical measurement.

(2) Noise Analysis

Due to the limited sampling number, the peak/valley position of discrete signal may not be exactly the same as that of continuous signal (Fig. 4, $m = 0.5, 1, 1.5$), resulting in signal frequency variations (Table 2).

Furthermore, the noise (air turbulence, environmental vibration, instrument noise, etc.) may distort the interferometric signal. As a result, the peak/valley position of the

signal may be shifted (Fig. 5, $m = 0.5, 2.5$), causing signal frequency fluctuations; and the false peak/valley of the signal may be generated (Fig. 5, $m = 1, 1.5$), yielding signal false frequencies (Table 2).

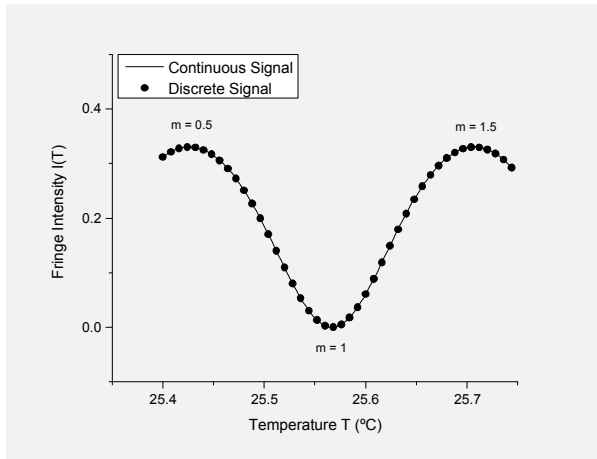


Figure 4 Signal peak/valley position is affected by limited sampling number

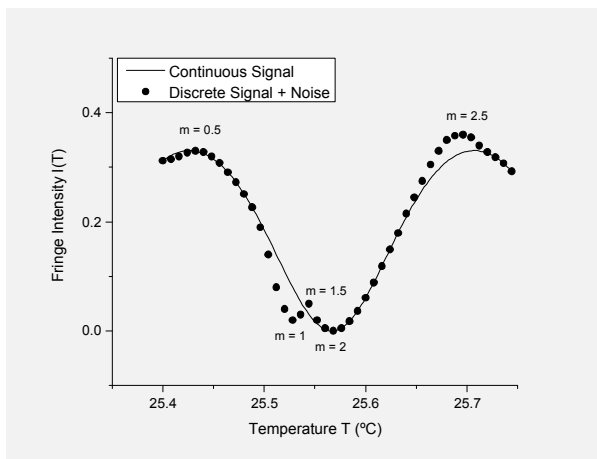


Figure 5 Signal peak/valley position is affected by the noise

Table 2 Signal frequency change caused by inaccurate peak/valley position and false peak/valley information

	Continuous Signal			Discrete Signal			Discrete Signal + The Noise				
m	0.5	1.0	1.5	0.5	1.0	1.5	0.5	1.0	1.5	2.0	2.5
$T(^{\circ}\text{C})$	25.426	25.567	25.707	25.424	25.568	25.704	25.432	25.528	25.544	25.568	25.696
$f(\text{K}^{-1})$		3.55	3.57		3.47	3.68		5.21	31.25	20.83	3.91

Shown in Table 2, the false frequency is the major factor that will affect the measurement accuracy. Choosing a lower sampling rate may bring about more frequency variations (Fig. 6) and fluctuations (Fig. 7) but less false frequencies. Fig. 7 shows that, with given test conditions, a sampling rate below 500 sample/K was suitable for ethanol to avoid the false frequencies. However, it is time consuming to find an optimised sampling rate for different materials under different test conditions. Furthermore, because the noise was randomly distributed, a manual false frequency removal was often required even at lower sampling rate.

To reduce the frequency variations and fluctuations while eliminating the false frequencies, the frequency structures of the signal and noise have been analyzed and a methodology has been developed for accurate dn/dT measurement. With this methodology, a higher sampling rate is utilized to restrain the frequency variations and fluctuations, while an FFT low-pass filter is employed to block the false frequencies.

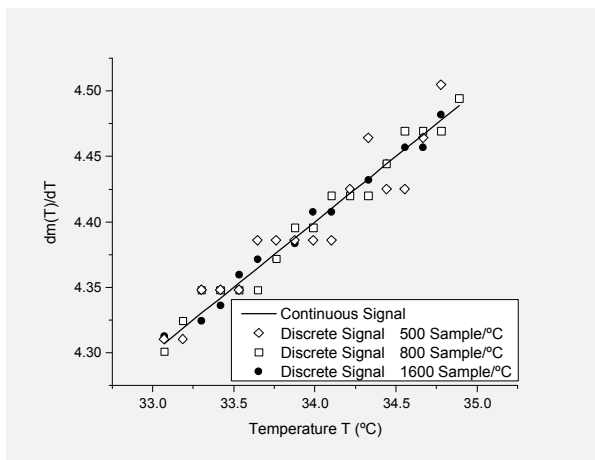


Figure 6 Signal frequency ($f = m' = dm/dT$) derived from the simulation signal [Eq. (10)] at different sampling rate. Lower sampling rate will bring about more frequency variations

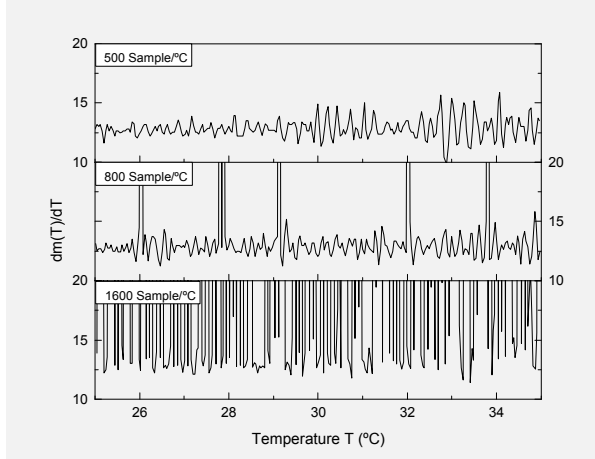


Figure 7 Signal frequency ($f = m' = dm/dT$) derived from the measured signal (anhydrous ethanol) at different sampling rate. Lower sampling rate will bring about more frequency fluctuations but less false frequencies

(3) Frequency Analysis

The frequency structures of the signal [Eq. (9)] and noise (Fig. 5) are shown in Fig. 8a, in which the average frequency $\bar{f} = 4K^{-1}$ and frequency change $\Delta f = 1K^{-1}$ [Eqs. (13) & (14)]. Some frequency fluctuations and all false frequencies (Table 2) are higher than the maximum signal frequency $\bar{f} + \Delta f/2 = 4.5K^{-1}$.

The fringe intensity $I(T)$ described by Airy's formula can be transformed to its spectrum magnitude $\hat{I}(f) = \mathcal{F}[I(T)]$ by FFT [10] (Fig. 8b).

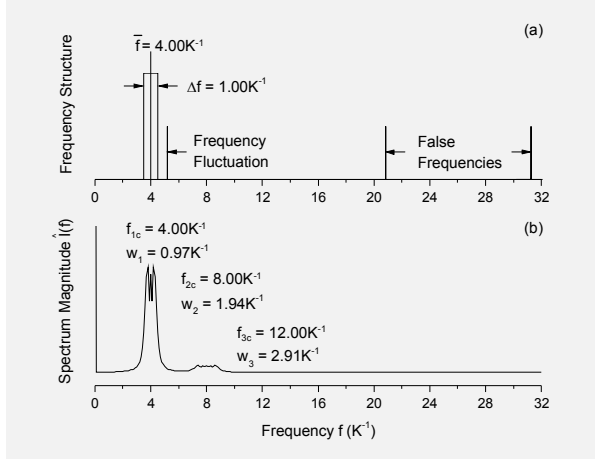


Figure 8 (a) The frequency structures of simulation signal and noise (b) The spectrum magnitude of the simulation signal obtained by FFT

Fig. 8 shows that the average frequency is related to the center frequencies f_{qc} of q th spectrum harmonic components,

$$\bar{f} \approx f_{1c} = f_{2c}/2 = f_{3c}/3 = f_{qc}/q = 4.00K^{-1}, \quad (17)$$

while the frequency change is related to the full width at half maximum (FWHM) w_q of q th spectrum harmonic components,

$$\Delta f \approx w_1 = w_2/2 = w_3/3 = w_q/q = 0.97K^{-1}. \quad (18)$$

Fig. 9 and Table 3 provide more information about the relationship between signal frequency structure and signal spectrum magnitude obtained by FFT. With the decrease of FWHM, the spectrum peak is getting sharper and dm/dT becomes a constant.

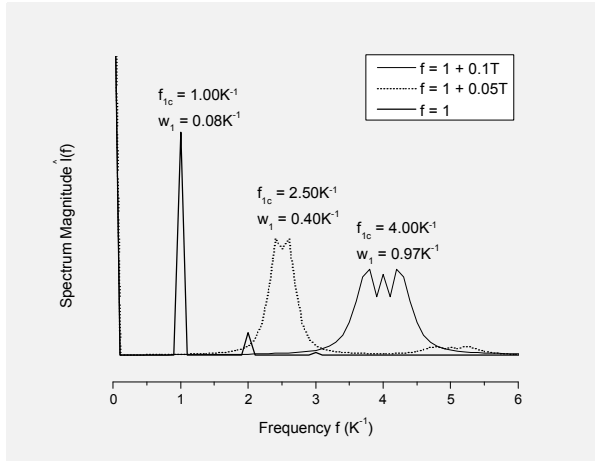


Figure 9 The spectrum magnitude of the simulation signal with different simulation parameter ($a = 0, 0.05, 0.1K^{-2}$)

Table 3 The center frequency and FWHM of spectrum fundamental component corresponding to different simulation parameter ($a = 0, 0.05, 0.1K^{-2}$)

T_0	T_N	ΔT	\bar{T}	b	a	$f = b + aT$	$\bar{f} = b + a\bar{T}$	f_{1c}	$\Delta f = a\Delta T$	w_1
25 °C	35 °C	10 °C	30 °C	1 K ⁻¹	0.10 K ⁻²	1.0 + 0.10T	4.0 K ⁻¹	4.0 K ⁻¹	1.0 K ⁻¹	0.97 K ⁻¹
					0.05 K ⁻²	1.0 + 0.05T	2.5 K ⁻¹	2.5 K ⁻¹	0.5 K ⁻¹	0.40 K ⁻¹
					0	1.0 K ⁻¹	1.0 K ⁻¹	1.0 K ⁻¹	0	0.08 K ⁻¹

Based on the above discussion, it can be concluded that: 1. The frequency structure of $I(T)$ is contained in the fundamental component of $\hat{I}(f)$. 2. Some frequency fluctuations and all false frequencies go beyond the fundamental component of $\hat{I}(f)$. 3. An FFT low-pass filter can be applied to $I(T)$ to keep the frequency structure but restrain frequency fluctuations and eliminate false frequencies. Consequently, a methodology for accurate dn/dT measurement can be summarized as follows: 1. Apply FFT to transform $I(T)$ to $\hat{I}(f)$ and find f_{1c} and w_1 to determine the cut-off frequency of an FFT low-pass

filter ($f_{cutoff} > f_{1c} + w_1/2$). 2. Employ the filter to remove the noise from $I(T)$. 3. Perform peak analysis to derive dn/dT from the noise-removed $I(T)$.

4. Experimental Results and Discussion

The methodology for accurate dn/dT measurement was tested against anhydrous ethanol and de-ionized water. In the experiments, the signal sampling rate was 800 samples/°C and the observation temperature range was 25~35 °C.

The interferometric signals measured with ethanol and water are shown in Figs. 10(a) & 13(a); and the signal frequencies $f = dm(T)/dT$ derived from the measured signals $I_r(T)$ by peak analysis are shown in Figs. 11(a) & 14(a). The noise superimposed on the signal [Figs. 10(a) & 13(a)] brought about frequency fluctuations and false frequencies [Figs. 11(a) & 14(a)].

The signal spectrums $\hat{I}(f)$ transformed from the measured signals $I_r(T)$ by FFT are shown in Figs. 12 & 15. Comparing Fig. 12 with Fig. 15, the average frequency ($\bar{f} \approx f_{1c}$) of ethanol is higher than that of water and the frequency change ($\Delta f \approx w_1$) of ethanol is smaller than that of water, indicating that the dn/dT of ethanol is larger but nearly a constant, while that of water is smaller but more temperature dependent. By FFT low-pass filtering, the noise was removed thoroughly from the measured signals [Figs. 10(b) & 13(b)], and the frequency fluctuations were restrained and false frequencies were blocked [Figs. 11(b) & 14(b)].

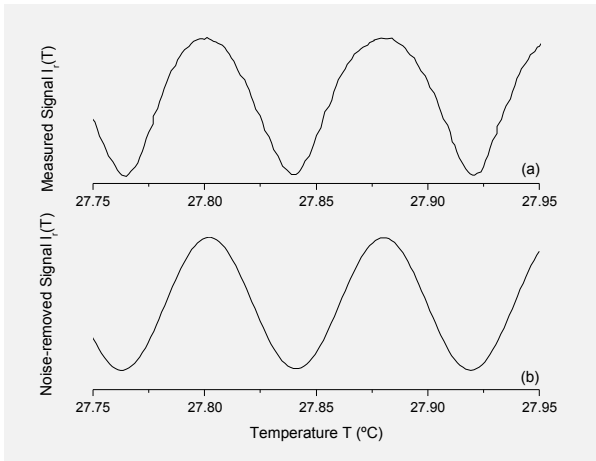


Figure 10 (a) The interferometric signal $I_r(T)$ measured with ethanol. (b) The noise-removed signal $I_r(T)$

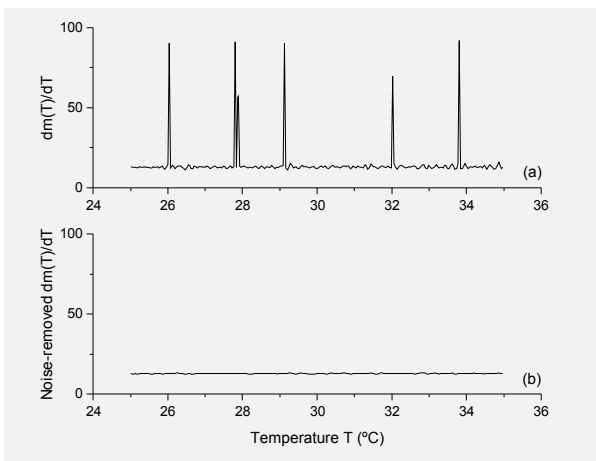


Figure 11 (a) The signal frequency $dm(T)/dT$ derived from the interferometric signal $I_r(T)$ measured with ethanol. (b) The signal frequency $dm(T)/dT$ derived from the noise-removed signal $I_r(T)$

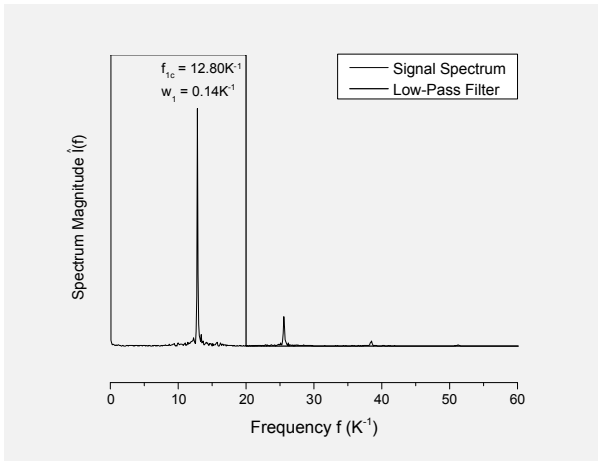


Figure 12 The signal spectrum $\hat{I}(f)$ transformed from the interferometric signal $I_r(T)$ measured with ethanol.

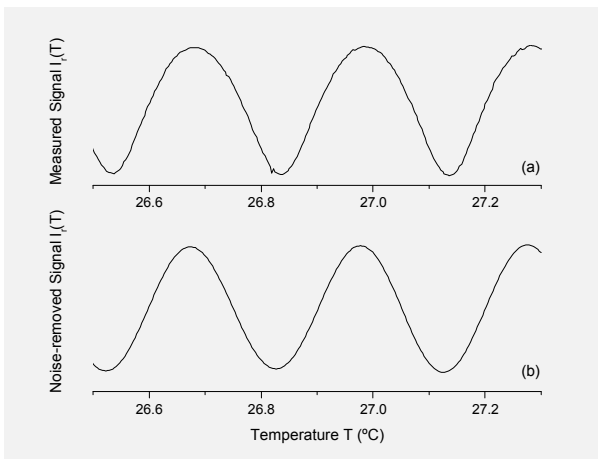


Figure 13 (a) The interferometric signal $I_r(T)$ measured with water. (b) The noise-removed signal $I_r(T)$

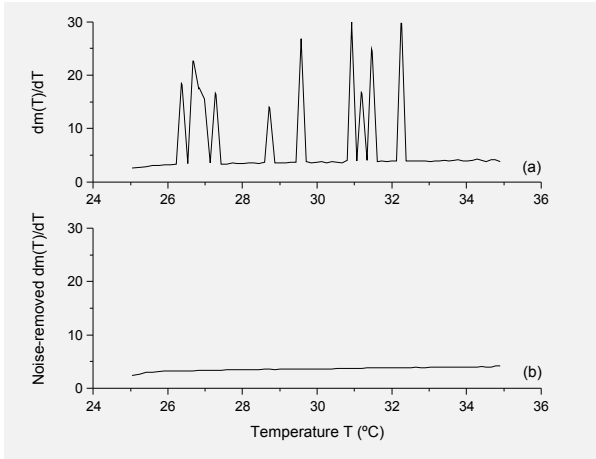


Figure 14 (a) The signal frequency $dm(T)/dT$ derived from the interferometric signal $I_r(T)$ measured with water. (b) The signal frequency $dm(T)/dT$ derived from the noise-removed signal $I_r(T)$

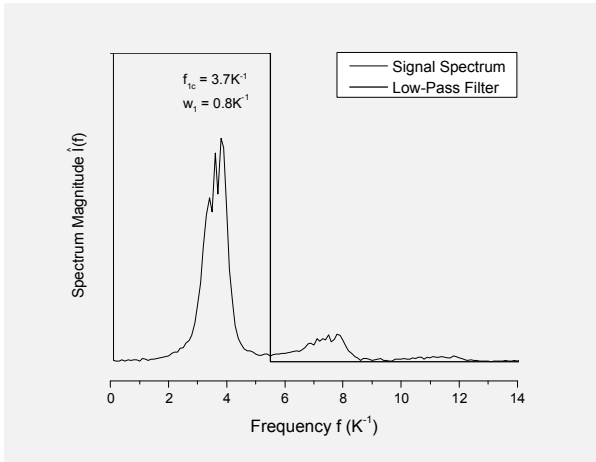


Figure 15 The signal spectrum $\hat{I}(f)$ transformed from the interferometric signal $I_r(T)$ measured with water.

The experimental results are summarized in Table 4. The dn/dT values over the observation temperature range 25~35°C may be found in the derived equations, and the measured data are in very good agreement with the literature values [11]. This agreement

demonstrates that accurate results can be achieved with this method. Moreover, the standard deviations are only about 0.075% and 1.03% of the measured mean values of ethanol and water, respectively, exhibiting high precision.

Table 4 Parameters for material thermophysical property characterization across the observation temperature range 25~35°C

Sample	Frequency Parameter (K^{-1})			$-dn/dT$ ($\times 10^{-4}K^{-1}$)		
	$\bar{f} \approx f_{1c}$	$\Delta f \approx w_1$	$\Delta f/\bar{f}$	25~35 °C	25 °C ^a	25 °C (Literature) ^b
Ethanol	12.8	0.14	1.1%	$3.90 + 0.005T$	4.025 ± 0.003	4.02
Water	3.7	0.8	22%	$0.12 + 0.034T$	0.97 ± 0.01	0.99

^a mean value of ten measurements ^b Reference 11

Up to now, the thermal expansion of solid material and the temperature effect of quartz cuvette containing gas or liquid material have not been taken into consideration in Eq. (3). For an isotropic transparent solid with two parallel surfaces, considering the contribution of material thickness change to the interferometric signal, Eq. (3) can be expressed as:

$$\Delta s = 2n(T)L(T). \quad (19)$$

$$f = \frac{dm}{dT} = \frac{d}{dT} \left(\frac{\Delta s}{\lambda} \right) = \frac{2}{\lambda} \left(L \frac{dn}{dT} + \frac{dL}{dT} n \right). \quad (20)$$

The thickness change of solid material due to the thermal expansion can be expressed as:

$$\frac{dL}{dT} = \alpha L. \quad (21)$$

α is the linear thermal expansion coefficient, we have

$$f = \frac{2L}{\lambda} \left(\frac{dn}{dT} + \alpha n \right). \quad (22)$$

The measured signal frequency contains the component contributed by sample refractive index change and that contributed by sample thickness change. Defining the temperature coefficient of optical path length

$$\frac{dS}{dT} = \frac{\lambda}{2L} f = \frac{dn}{dT} + \alpha n, \quad (23)$$

the measured signal frequency can be used for characterizing the thermophysical property of transparent solid materials, such as optical glasses, within a large observation temperature range [5].

For the gas or liquid enclosed in a transparent quartz cuvette, the Fabry-Perot interferometer actually consists of three layers with four parallel surfaces (S_1, S_2, S_3, S_4): the front cuvette wall ($S_1 \sim S_2$), the sample in the cuvette ($S_2 \sim S_3$), and the rear cuvette wall ($S_3 \sim S_4$). The measured temperature-dependent interferometric signal can be considered a superposition of six interferometric signals with different free spectral ranges ($S_1 \sim S_2, S_1 \sim S_3, S_1 \sim S_4, S_2 \sim S_3, S_2 \sim S_4, S_3 \sim S_4$), Eq. (3) can be expressed as:

$$\Delta S_{12} = 2(n_{Si}l), \quad (24)$$

$$\Delta S_{13} = 2(n_{Si}l + nL), \quad (25)$$

$$\Delta S_{14} = 2(n_{Si}l + nL + n_{Si}l), \quad (26)$$

$$\Delta S_{23} = 2(nL), \quad (27)$$

$$\Delta S_{24} = 2(nL + n_{Si}l), \quad (28)$$

$$\Delta S_{34} = 2(n_{Si}l), \quad (29)$$

Refer to Eqs. (20) ~ (22), these differences of optical path length generate six interferometric signals with different signal frequency:

$$f_{12} = f_{Si}, \quad (30)$$

$$f_{13} = f_{dn/dT} + f_{Si}, \quad (31)$$

$$f_{14} = f_{dn/dT} + 2f_{Si}, \quad (32)$$

$$f_{23} = f_{dn/dT}, \quad (33)$$

$$f_{24} = f_{dn/dT} + f_{Si}, \quad (34)$$

$$f_{34} = f_{Si}, \quad (35)$$

$$f_{dn/dT} = \frac{2L}{\lambda} \frac{dn}{dT}, \quad (36)$$

$$f_{Si} = \frac{2l}{\lambda} \left(\frac{dn_{Si}}{dT} + \alpha_{Si} n_{Si} \right). \quad (37)$$

Here $l = 1 \text{ mm}$, $n_{Si} = 1.46$, $dn_{Si}/dT = 1.01 \times 10^{-5} K^{-1}$, and $\alpha_{Si} = 1.83 \times 10^{-7} K^{-1}$ are the wall thickness, refractive index, temperature coefficient of refractive index, and linear thermal expansion coefficient of the fused-quartz cuvette, respectively [12, 13]. $f_{dn/dT}$ is the frequency component contributed by sample refractive index change, while f_{Si} is the frequency component contributed by cuvette temperature effect. The ratio

$$\gamma = \frac{f_{Si}}{f_{dn/dT}} = \frac{l}{L} \frac{\frac{dn_{Si}}{dT} + \alpha_{Si} n_{Si}}{\frac{dn}{dT}} = \frac{1}{10} \frac{1.01 \times 10^{-5} + 2.67 \times 10^{-7}}{|dn/dT|} = \frac{1.04}{|dn/dT| \times 10^4} \% \quad (38)$$

In the case of distilled water, $dn/dT = -0.99 \times 10^{-4} K^{-1}$ and $\gamma = 1.05\%$. Most liquid samples have higher $|dn/dT|$ values than distilled water. For example, in the case of ethanol, $dn/dT = -4.02 \times 10^{-4} K^{-1}$ and $\gamma = 0.26\%$. The cuvette is designed to have thin walls ($l = 1 \text{ mm}$) but a thick sample ($L = 10 \text{ mm}$) for minimizing its temperature effect on the interferometric signal. $f_{12} = f_{34} = f_{Si}$ is almost a DC signal and will not affect the peak analysis accuracy, while f_{13} , f_{14} , and f_{24} may cause some negligible frequency shift from $f_{23} = f_{dn/dT}$, thus the measured signal frequency is

$$f \cong f_{dn/dT} = \frac{2L}{\lambda} \frac{dn}{dT}. \quad (39)$$

Since the signal frequency is associated with the change of optical path length [Eq. (20)], it is convenient to analyse the temperature-dependent interferometric signals in frequency domain and investigate the frequency components contributed by different factors, such as sample refractive index change, sample thermal expansion, and cuvette temperature effect.

For transparent solid material, the signal frequency is associated with the temperature coefficient of optical path length [Eq. (23)], while for gas or liquid material, the signal frequency is associated with the temperature coefficient of refractive index [Eq. (39)]. Therefore, it is convenient to utilize signal frequency parameters to characterize material thermophysical property. Furthermore, by real-time FFT, the signal frequency and thus the material dS/dT or dn/dT can be acquired instantly, which will be presented in a later work. The methodology described in this paper may be used to build an instrument to monitor changes in the thermophysical property of process materials. It is envisioned that this instrument may have value for process control applications or quality control inspections.

5. Conclusion

The method of frequency analysis for dn/dT measurement has been developed and tested for ethanol and water. For accurate and precise dn/dT measurements, frequency analysis needs to be performed before conducting peak analysis to remove the noise from the measured interferometric signal. By FFT, a low-pass filter can be designed and employed to restrain frequency fluctuations and eliminate false frequencies. The experimental results show that the method can work at any sampling rate with different

materials. The signal processing is simple, the noise reduction is effective, and the measured data are accurate and precise across the observation temperature range. With the method developed in this work, we are able to examine material interferometric signal from another perspective and characterize material thermophysical property with signal frequency parameters. The method lays the foundation for real-time monitoring or process control using dn/dT measurement.

6. Acknowledgment

Financial support from the Government of Canada's ecoENERGY Innovation Initiative (ecoEII), project EETR-015, is gratefully acknowledged.

References

- [1] M.P.P. Castro, A.A. Andrade, R.W.A. Franco, P.C.M.L. Miranda, M. Sthel, H. Vargas, R. Constantino, M.L. Baesso, *Chem. Phys. Lett.* 411 (2005) 18
- [2] J. Shen, N.G.C. Astrath, P.R.B. Pedreira, F.B. Guimarães, R. Gieleciak, Q. Wen, K.H. Michaelian, C. Fairbridge, L.C. Malacarne, J.H. Rohling, M.L. Baesso, *Fuel* 163 (2016) 324
- [3] Q. Wen, J. Shen, Z. Shi, E. Dy, K.H. Michaelian, C. Fairbridge, N.G.C. Astrath, J.H. Rohling, M.L. Baesso *Chem. Phys. Letters* 539 (2012) 54
- [4] T.Y. Fan, J.L. Daneu, *Appl. Opt.* 37 (1998) 1635
- [5] A. Steimacher, A.N. Medina, A.C. Bento, J.H. Rohling, M.L. Baesso, *J. Non-Crystalline Solids* 348 (2004) 240
- [6] M.L. Baesso, J. Shen, R.D. Snook, *J. Appl. Phys.* 75 (1994) 3732
- [7] A.A. Andrade, T. Catunda, I. Bodnar, J. Mura, M.L. Baesso, *Rev. Sci. Instrum.* 74 (2003) 877
- [8] M. Daimon, A. Masumura, *Appl. Opt.* 46 (2007) 3881
- [9] M. Born, E. Wolf, *Principles of Optics*, Cambridge University Press, 1997
- [10] J. Proakis, D. Manolakis, *Digital Signal Processing*, Prentice-Hall, 1996
- [11] G. Abbate, A. Attanasio, U. Bemini, E. Ragozzino, F. Somma, *J. Phys. D: Appl. Phys.* 9 (1976) 1945
- [12] R.C. Weast, M.J. Astle, W.H. Beyer, *CRC Handbook of Chemistry and Physics*, 69th Edition, CRC Press, Inc., Boca Raton, 1988-1989
- [13] W.S. Rodney, R.J. Spindler, *Journal of Research of the National Bureau of Standards*, 53 (1954) 185